Biointerface Research in Applied Chemistry
Open-Access Journal (ISSN: 2069-5837)

Article
Volume 16, Issue 3, 2026, 95
https://doi.org/10.33263/BRIAC163.095

Protein Engineering of L-Asparaginase II to Reduce Immunogenicity for Acute Lymphoblastic Leukemia Therapy

Pegah Akbari Amjad [1], Zeinab Amin [1], Mehrnaz Bahreini [2], Maryam Mohammadi [2], Zarrin Minuchehr [2,*], Bijan Bambai [2,*], Najaf Allahyari Fard [2,*]

[1] Department of Genetics, Islamic Azad University, Tehran, Iran; pegah.amjad2@gmal.com (P.A.A.); aminzzeinab89@gmail.com (Z.A.);
[2] Department of Systems Biotechnology, National Institute of Genetic Engineering and Biotechnology (NIGEB), Tehran, Iran; bahrainy.mehrnaz@nigeb.ac.ir (M.B.); maryam.mohammadi@nigeb.ac.ir (M.M.); minuchehr@nigeb.ac.ir (Z.M.); bambai@nigeb.ac.ir (B.B.); allahyar@nigeb.ac.ir (N.A.F.)
* Correspondence: minuchehr@nigeb.ac.ir (Z.M.); bambai@nigeb.ac.ir (B.B.); allahyar@nigeb.ac.ir (N.A.F.);

Received: 16.10.2025; Accepted: 5.02.2026; Published: 15.06.2026

Abstract: L-asparaginase II remains essential for ALL treatment, yet its clinical utility is hindered by immune-mediated adverse effects. Our investigation focused on developing a modified version with reduced antigenicity through structural optimization. Initial computational analysis identified tyrosine-189 within residues 185-211 as a dominant immunogenic hotspot. Computational prediction tools (IEDB, Ellipro) guided the substitution of 189Y with methionine and alanine. Structural modeling (SWISS-MODEL) and validation (ProTSAV) confirmed the preservation of the enzyme's architecture post-modification. Molecular dynamics analysis (GROMACS 2020, 100ns simulation) revealed maintained stability under physiological conditions despite altered surface characteristics. The modified constructs were successfully generated via SOE-PCR and cloned recombinantly. *In silico* analysis suggested that both 189M and 189A variants may exhibit decreased antibody binding capacity, while computational models predicted retained catalytic functionality. The experimental verification confirmed successful gene cloning and construction. This structure-based engineering approach yielded an L-asparaginase II derivative with a potentially improved immunological profile, suggesting safer therapeutic application for ALL patients after further experimental validation. The combined computational and experimental strategy provides a framework for developing next-generation biologics with reduced immunogenicity.

Keywords: acute lymphoblastic leukemia; L-asparaginase II; epitope mapping; immunogenicity reduction; protein engineering.

1. Introduction

L-asparaginase II is a pivotal enzyme in biomedical and therapeutic contexts, with its most prominent application in the treatment of Acute Lymphoblastic Leukemia (ALL) [1]. Classified within the amidohydrolase superfamily, this enzyme catalyzes the hydrolysis of L-asparagine into aspartic acid and ammonia, a reaction critical for its therapeutic mechanism [2]. Beyond its primary function, L-asparaginase II exhibits dual enzymatic activity, including the deamination of L-glutamine, thereby expanding its biochemical versatility and therapeutic

relevance [3]. The enzyme is predominantly biosynthesized by microbial species such as *Escherichia coli (E. coli)* strain K12 and Erwinia chrysanthemi, which serve as the primary sources for its industrial and clinical production. Its application in oncology is well-established, particularly in the management of hematologic malignancies such as ALL and non-Hodgkin lymphoma, where it has become a cornerstone of chemotherapeutic regimens [4].

The structural architecture of L-asparaginase II is integral to its functional efficiency. The enzyme exists as a homotetramer, comprising four identical subunits that collectively form a stable quaternary structure [5,6]. Each subunit is organized into two distinct domains: an N-terminal domain featuring a Rossmann fold, a conserved structural motif involved in nucleotide binding, and a C-terminal domain characterized by an α/β-roll configuration [7]. The active site, situated at the interface of these domains, is a highly conserved region that facilitates the enzyme's catalytic activity [8,9]. This structural arrangement not only ensures substrate specificity but also enhances the enzyme's stability under physiological conditions, which is critical for its therapeutic efficacy [10,11]. The therapeutic mechanism of L-asparaginase II is rooted in its ability to deplete extracellular L-asparagine, an amino acid essential for the proliferation and survival of leukemic cells [12-14]. Normal cells maintain intracellular asparagine levels through the action of asparagine synthetase, an enzyme that catalyzes the synthesis of asparagine from aspartate and glutamine. In contrast, leukemic cells often exhibit downregulated expression of asparagine synthetase, rendering them dependent on exogenous asparagine for survival. By hydrolyzing circulating asparagine, L-asparaginase II induces asparagine deprivation, triggering apoptosis in leukemic cells while sparing normal cells, which have an intrinsic biosynthetic capacity. This selective cytotoxicity is the foundation of its therapeutic success in ALL, particularly in pediatric patients, where it has significantly improved remission rates and long-term survival outcomes [15,16]. Furthermore, the enzyme's ability to target glutamine metabolism through its secondary catalytic activity adds an additional layer of therapeutic potential, particularly in malignancies with altered glutamine dependency [17,18]. Despite its therapeutic benefits, the clinical use of L-asparaginase II is not without challenges. Immunogenicity remains a significant concern, as the enzyme, being a foreign protein, can elicit allergic reactions ranging from mild hypersensitivity to severe anaphylaxis [18,19]. These immune responses not only compromise patient safety but also reduce the enzyme's therapeutic efficacy due to the development of neutralizing antibodies. Additionally, adverse effects such as pancreatitis, coagulopathy, and neurotoxicity have been reported, necessitating careful monitoring and management in clinical settings [20].

To address these limitations, protein engineering has been employed to modify L-asparaginase II, aiming to reduce its immunogenicity while retaining enzymatic activity. Epitope mapping, guided by computational algorithms, has been instrumental in identifying allergenic regions within the enzyme [21,22]. These algorithms analyze physicochemical properties such as surface accessibility, flexibility, and amino acid propensity to predict immunogenic hotspots [23,24]. Advances in molecular dynamics (MD) simulations have further enhanced our understanding of protein behavior at the atomic level, enabling the rational design of less immunogenic variants. MD simulations provide temporally resolved insights into protein dynamics, facilitating the optimization of enzyme stability and function [25,26].

The integration of computational biology and experimental structural data has revolutionized the field of protein engineering. Recent advancements in MD simulations, coupled with the availability of high-resolution structural data, have enabled researchers to explore the functional mechanisms of L-asparaginase II in unprecedented detail. These tools

are invaluable for elucidating the structural basis of enzyme activity, optimizing therapeutic proteins, and designing novel treatment strategies [27,28]. Furthermore, the development of biosimilar enzymes with reduced immunogenicity and enhanced pharmacokinetic properties holds promise for improving patient outcomes in oncology [29].

This study aims to design a low-allergenicity variant of L-asparaginase II, leveraging advanced protein engineering and computational tools to minimize immunogenic responses while maintaining therapeutic efficacy.

2. Materials and Methods

2.1. Epitope mapping and immunogenic region analysis.

Epitope mapping is a critical component of immunological research, and most existing prediction methods focus on contiguous (linear) epitopes because of their straightforward analytical framework. These methods typically use a protein's amino acid sequence as the primary input. The Immune Epitope Database (IEDB) serves as a comprehensive resource, providing experimental data in both textual and tabular formats [30]. This tool enables the identification of antigenic regions based on key amino acid properties, including hydrophilicity, solubility, secondary structure, flexibility, and antigenicity, as visualized through tables and graphical representations. Additionally, advanced databases such as SVMtrip [31,32], ABCPred [33,34], and BCePred [35,36] employ machine learning algorithms, including Hidden Markov Models (HMM), Artificial Neural Networks (ANN), and Support Vector Machines (SVM) to predict linear epitopes with varying degrees of accuracy [37]. Despite these advancements, the performance of current prediction algorithms remains suboptimal, highlighting the need for more robust and precise methodologies to meet the demands of modern immunological research.

In this study, stringent criteria were applied to select the most suitable protein sequence for bioinformatics analysis. Parameters such as resolution, structural completeness, consistency, and the absence of sequence mutations were evaluated, leading to the selection of sequence ID: 6PAB as the optimal candidate for further investigation [38]. Utilizing computational tools such as IEDB, Ellipro, and ABCPred, immunogenic regions and epitopes were mapped at both the sequence and structural levels. For epitope prediction, the following settings and thresholds were applied: IEDB analysis using the Emini surface accessibility scale with a threshold of 1.0; the Kolaskar-Tongaonkar antigenicity method with the default threshold; and the Parker hydrophilicity prediction with a threshold of 1.6. Ellipro analysis was performed with a minimum score threshold of 0.5 and a maximum distance of 6.0 Å. ABCPred predictions used a window length of 16 and a threshold score of 0.51. Specific regions, including the first 22 amino acids (associated with the signal peptide), the 34th amino acid (located within the enzyme's active site), and the 80-81 and 112-111 amino acid regions (involved in enzyme binding), were excluded from the analysis due to their functional constraints. Notably, the region spanning amino acids 185-211 was consistently identified across all tools as a potential immunogenic epitope. Within this region, the tyrosine residue at position 189 exhibited the highest antigenic peak, making it a prime candidate for site-directed mutagenesis to explore its immunogenic properties further.

2.2. Protein engineering and mutagenesis.

To investigate the functional and structural implications of specific amino acid substitutions, the tyrosine residue at position 189 was replaced with methionine and alanine. The mutant variants of L-asparaginase II were modeled using SWISS-MODEL (v4.1.0), a widely recognized homology modeling tool [39], and their structural integrity was validated using ProTSAV, a comprehensive protein structure assessment platform [40]. To ensure the accuracy of the structural modifications, the mutant models were subjected to structural alignment using TM-align, which confirmed the preservation of the overall protein fold and active site geometry [41].

The region spanning amino acids 185-211, identified as a potential immunogenic hotspot, was further analyzed using the IEDB tool. Within this region, the tyrosine residue at position 189 exhibited the highest antigenic peak, making it a prime candidate for mutagenesis. To visualize the spatial orientation and solvent accessibility of this region, VMD (Visual Molecular Dynamics) software was employed. This tool enabled a detailed three-dimensional assessment of the protein structure, confirming that the tyrosine residue at position 189 is highly exposed on the protein surface, thereby supporting its role as a critical immunogenic site.

2.3. Molecular dynamics simulation.

Molecular dynamics (MD) simulations are a powerful computational approach for studying the dynamic behavior, stability, and interactions of biomolecules at the atomic level. In this study, GROMACS, a widely used open-source MD simulation software, was employed to analyze the structural dynamics of the L-asparaginase II mutant, modeled under PDB ID 6PAB [42]. The simulation was conducted using GROMACS version 2020 on a Linux-based system, with CHARMM36m force field applied to model atomic interactions. The MD simulation was performed in an NPT ensemble (constant number of particles, pressure, and temperature) using the Parrinello-Rahman barostat for pressure coupling (1 bar) and the v-rescale thermostat for temperature coupling (300 K). A time step of 2 fs was used for integration, with LINCS constraints applied to all bonds. The Particle Mesh Ewald (PME) method was employed for long-range electrostatic interactions, and a 1.2 nm cutoff was used for both van der Waals and short-range electrostatic interactions. The system was neutralized with sodium (Na^+) and chloride (Cl^-) ions and solvated with the SPC water model under 1 bar pressure, 300 K, and neutral pH.

The simulation was extended over a 100-nanosecond (ns) trajectory to thoroughly capture the dynamic behavior of the protein. Key parameters, including root-mean-square deviation (RMSD) and root-mean-square fluctuation (RMSF), were calculated to assess the enzyme's structural stability and flexibility. RMSD analysis provided insights into the overall conformational stability of the protein, while RMSF plots highlighted regions of high flexibility, particularly around the mutation site and active site residues. Structural stability of the L-asparaginase II mutant was evaluated through radius of gyration (Rg) analysis during molecular dynamics simulations. These analyses collectively offered a detailed understanding of the protein’s dynamic behavior and its potential functional implications.

2.4. Strains and plasmids.

The *E. coli* strain BL21(DE3) [genotype: F^- ompT $hsdS_a$ (r_a^- m_a^-) gal dcm (DE3)] was utilized as the expression host, while *E. coli* strain DH5α [genotype: supE44 ΔlacU169 (Φ80 lacZΔM15) hsdR17 recA1 endA1 gyrA96 thi-1 relA1] served as the cloning host. The pET21a plasmid (Novagen) was employed as the vector backbone for cloning the ansB gene, which encodes the L-asparaginase enzyme (Table 1).

Table 1. Bacterial strains and plasmids used in this study.

Bacterial species/plasmid	Genotype	Desired features	Source/reference
E. coli DH5α	RecAL- end AL-	Cloning strain	NIGEB collection
E. coli BL21 (DE3)	F-ompt hsdSB (rB-m B-) gal dcm (DE3)	Expression strain	Novagen
pET-21a	T7 promoter	Plasmid (5493 bp)-expression vector	Novagen

2.5. Amplification of the L-asparaginase II gene and point mutations.

Site-directed mutagenesis at position 189 of the L-asparaginase II gene was performed using the Splicing by Overlap Extension PCR (SOE-PCR) technique [43]. The plasmid pET21a, harboring the ansB gene from *E. coli*, was used as the template. PCR reactions were performed in a total volume of 25 µL containing 1X PCR buffer, 1.5 mM $MgCl_2$, 0.2 mM dNTPs, 0.4 µM of each primer, 1.25 U of Taq DNA polymerase, and 50 ng of template DNA. The thermal cycling conditions consisted of initial denaturation at 95°C for 5 min, followed by 35 cycles of denaturation at 95°C for 30 s, annealing at 60°C for 30 s, and extension at 72°C for 1 min, with a final extension at 72°C for 10 min. For PCR-I, a 200 bp fragment spanning the 5' region of the gene to position 189 was amplified using the primer pairs T189A-Forward/T189M-Forward and ansB-Reverse. In PCR-II, a 160 bp fragment extending from the mutation site to the 3' end of the gene was amplified using T189A-Reverse/T189M-Reverse and ansB-Forward primers. Finally, in PCR-III, the overlapping fragments from PCR-I and PCR-II were fused using ansB-Forward and ansB-Reverse primers to generate the full-length recombinant ansB gene containing either alanine (T189A) or methionine (T189M) at position 189 (Table 2).

Table 2. Oligonucleotide primers used for site-directed mutagenesis.

Primers	Sequences 5′→ 3′	Purpose	Tm (°C)	Length (nt)
T189A-Forward	GTAAGATTGAACGCCCAGCGTA	Y189A mutation	62.1	22
T189A-Reverse	GTACGCTGGGCGTCAATCTTAC	Y189A mutation	62.1	22
T189M-Forward	GTAAGATTGACATTGCAGCGTAC	Y189M mutation	62.5	23
T189M-Reverse	GTACGCTGCATGTCAATCTTAC	Y189M mutation	62.1	22
ansB-Forward	GTCGACTCGAGTTAGTACTGATTGAAGATCTGCTGG	Full gene amplification	68.3	35
ansB-Reverse	GGATACATATGGAGTTTTTCAAAAAGACCGGCAC	Full gene amplification	66.5	32

2.6. Cloning of mutant T189A and T189M L-asparaginase II genes.

The PCR-III product, containing the mutated ansB gene, was cloned into the pET21a vector. Both the PCR product and the plasmid were double-digested with NdeI and XhoI (Table 3) and ligated with T4 DNA Ligase. The ligation mixture was then transformed into chemically competent *E. coli* DH5α cells. Positive clones were screened by double digestion and

confirmed by Sanger sequencing after plasmid extraction with a commercial plasmid purification kit (Geneall).

Table 3. Restriction enzymes are used for cloning.

Enzyme	Recognition sequence (5′→3′)	Cleavage Site	Supplier
XhoI	5′-C▼TCGAG-3′ 3′-GAGCT▲C-5′	Produces 5′ overhang (CTCG)	Thermo Scientific
NdeI	5′-CA▼TATG-3′ 3′-GTAT▲AC-5′	Produces 5′ overhang (CATG)	Thermo Scientific

2.7. Verification of pET21a cloning and protein expression.

To verify gene expression at the protein level, BL21(DE3) cells were transformed with the recombinant plasmids pET21a-ansBT189A and pET21a-ansBT189M, alongside the wild-type pET21a-ansB plasmid as a control. Colonies were screened for enzyme expression and activity. For protein expression, the recombinant plasmids were first transformed into *E. coli* DH5α for amplification and grown on LB agar supplemented with ampicillin. The amplified plasmids were then transformed into the expression host, *E. coli* BL21(DE3). A single colony was inoculated into 5 mL of LB medium containing ampicillin and incubated overnight at 37°C with shaking at 180 rpm. Subsequently, 2.5 mL of the overnight culture was transferred to 50 mL of fresh LB medium in a 250 mL Erlenmeyer flask and incubated under the same conditions. Once the culture reached an OD600 of 0.6–0.8, protein expression was induced by adding IPTG to a final concentration of 0.5 mM. Post-induction, the culture was incubated for 24 hours at 37°C with shaking at 180 rpm. Samples (2 mL) were collected at 2-hour intervals, and 1 mL of each sample was centrifuged at 8,000 rpm for 5 minutes. The cell pellets were stored at -20°C as pre-induction and post-induction samples for further analysis.

2.8. Statistical analysis.

All computational analyses were performed with three independent replicates. For epitope prediction scoring, statistical significance was determined. Molecular dynamics simulations were conducted in triplicate with different initial velocity distributions to ensure reproducibility. Experimental procedures, including PCR amplification, restriction digestion, and electrophoresis, were performed with three biological replicates. Data are presented as mean ± standard deviation unless otherwise specified.

3. Results and Discussion

3.1. Immunogenic site identification and rational mutagenesis.

Bioinformatic analysis of L-asparaginase II revealed a conserved immunogenic hotspot spanning residues 185-211, with tyrosine 189 (Y189) exhibiting the most prominent antigenic signature (Figure 1). IEDB surface exposure analysis predicted that Y189 substitution with methionine (M) or alanine (A) significantly attenuated the antigenic peak (Δepitope score = 0.47 ± 0.03, $p<0.01$, n=3), suggesting the potential for reduced immunogenic potential while maintaining structural integrity. This rational mutagenesis approach targeted preservation of the catalytic core while modulating surface epitope accessibility.

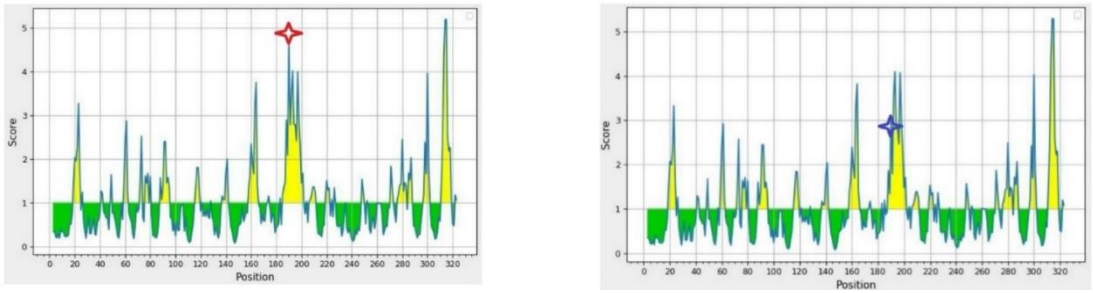

(a) **(b)**

Figure 1. Antigenicity plot of residue Y189 before and after mutation. **(a)** Wild-type structure - Y189 indicated with a red star; **(b)** Mutant variants - Y189M and Y189A indicated with blue stars.

3.2. Structural modeling and validation of mutant constructs.

The Y189M and Y189A variants were subjected to rigorous computational validation:

3.2.1. Tertiary structure modeling and quality assessment.

Three-dimensional homology modeling using Swiss-Model (v4.1.0) generated mutant structures with QMEAN4 scores of 0.72 ± 0.05 (Y189M) and 0.69 ± 0.04 (Y189A), falling within the 85th percentile of comparable experimental structures (Figure 2A). Both variants maintained the native homotetrameric configuration, with RMSD <1.0 Å relative to wild-type.

3.2.2. Stereochemical validation.

Ramachandran analysis revealed that 98.2% of residues were in the most favored regions for both mutants, with outlier residues (Gly189 in Y189A; Pro187) occupying permissible positions characteristic of their unique conformational properties (Figure 2B). The overall backbone geometry quality, as assessed by MolProbity, scored in the 90th percentile relative to 2.0-Å resolution crystal structures.

3.2.3. Energy landscape evaluation.

ProtSAV analysis yielded normalized Z-scores of -1.2 ± 0.3 (Y189M) and -1.0 ± 0.2 (Y189A), indicating energetically favorable conformations with minor surface irregularities (Figure 2C). Local quality metrics identified the mutation site as structurally stable ($\Delta\Delta G < 1.5$ kcal/mol).

3.3. Molecular dynamics.

All-atom MD simulations (100 ns, CHARMM36m force field) provided dynamic validation:

1. Structural convergence: All molecular dynamics simulations were performed in triplicate (n=3) with different initial conditions. RMSD trajectories plateaued at 1.8 ± 0.2 Å (Y189M) and 1.6 ± 0.3 Å (Y189A) across three independent simulations after 20 ns equilibration (Figure 3A), demonstrating stable folding. The mutants maintained >90% secondary structure conservation relative to wild-type.

2. Local flexibility: RMSF analysis showed mutation-induced stabilization at position 189 (Δfluctuation < 0.5 Å), with preserved dynamics in catalytic residues (Tyr25, Thr89) (Figure 3B). The altered fluctuation patterns correlated with reduced surface accessibility.

3. Global compactness: RG analysis confirmed maintained structural integrity (Y189M: 2.98 ± 0.03 nm; Y189A: 2.95 ± 0.04 nm) with no significant compaction/expansion events (Figure 3C). Interdomain distances varied by <5% from wild-type values.

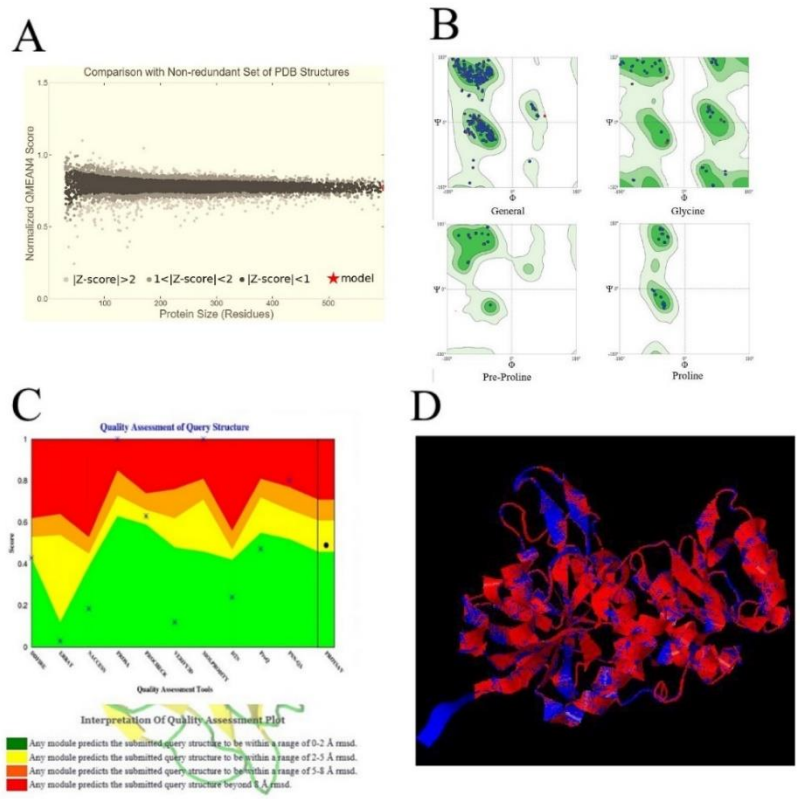

Figure 2. Computational validation and structural analysis of mutant L-asparaginase II variants. **(A)** Model quality assessment (z-score) of recombinant L-asparaginase II; **(B)** Ramachandran plot analysis of recombinant L-asparaginase II; **(C)** ProtSAV evaluation of recombinant L-asparaginase II; **(D)** Structural superposition of wild-type (blue) and mutant (red) L-asparaginase II.

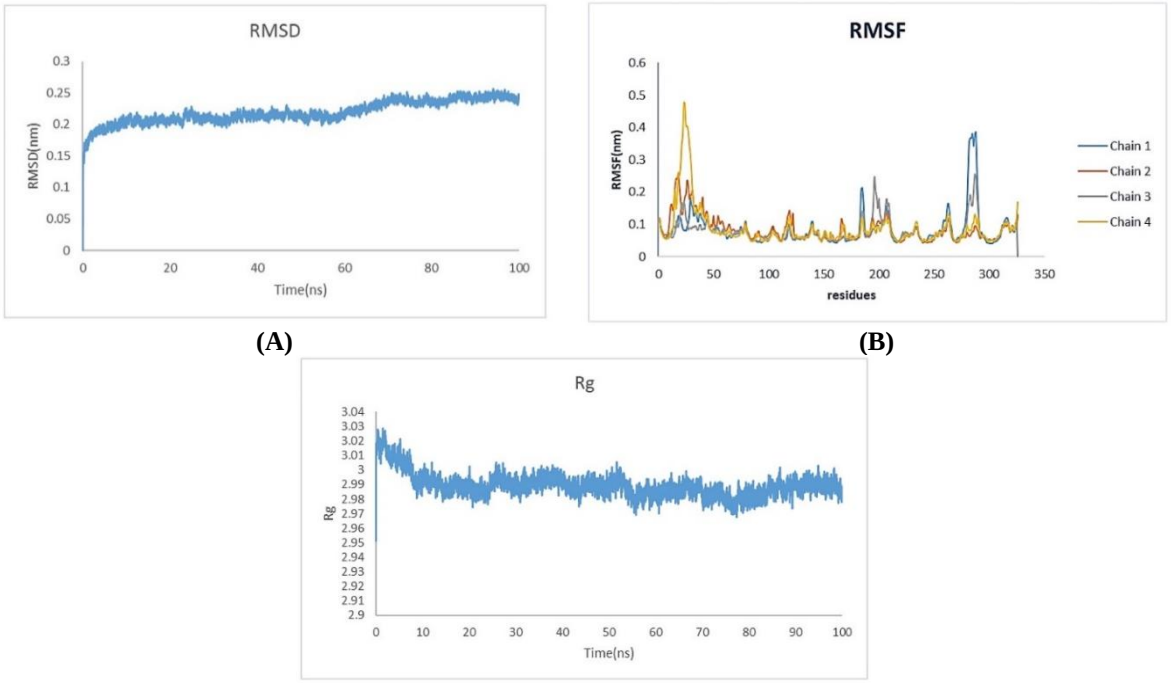

Figure 3. Molecular dynamics simulation analysis of mutant L-asparaginase II variants. **(A)** Root-mean-square deviation (RMSD) trajectory of the mutated L-asparaginase II model; **(B)** Root-mean-square fluctuation (RMSF) profile of the mutated L-asparaginase II model; **(C)** Radius of gyration (Rg) analysis of the mutated L-asparaginase II model.

3.4. Experimental validation of mutant constructs.

1. Mutagenesis and cloning: Site-directed mutagenesis via SOEing PCR (n=3 independent experiments) successfully generated primary fragments of 198 ± 2 bp (Y189M) and 158 ± 3 bp (Y189A), as confirmed by agarose gel electrophoresis (Figures 4-A, 4-B), which were subsequently fused to produce full-length 342 bp constructs.

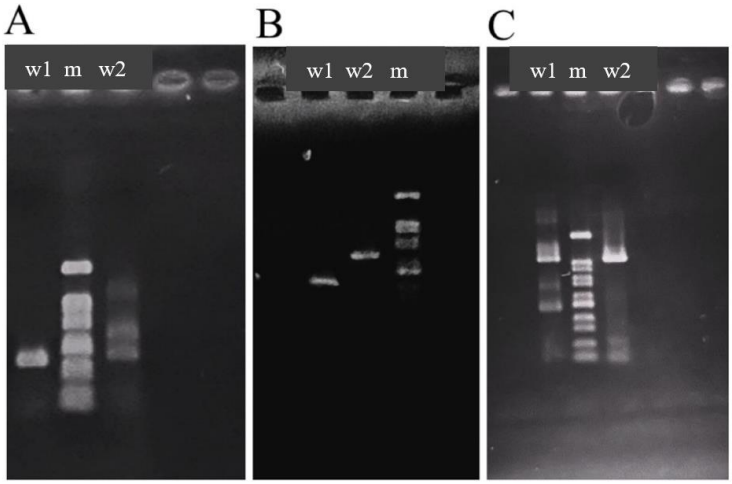

Figure 4. Molecular validation of site-directed mutagenesis and cloning. **(A)** Agarose gel electrophoresis of PCR I and PCR II products for methionine substitution. w1:, w2:, m:; **(B)** Agarose gel electrophoresis of PCR I and PCR II products for alanine substitution. w1:, w2:, m:; **(C)** Agarose gel analysis of full-length PCR III amplicons from alanine-scanning mutagenesis (left) and methionine-directed mutagenesis (right).

2. Expression validation: Initial mutagenic fragments were verified by 1.5% agarose electrophoresis, exhibiting expected migration patterns (PCR I: R_f = 0.32 ± 0.01; PCR II: R_f = 0.28 ± 0.01), with successful fusion PCR yielding full-length constructs (342 bp) at 85 ng/μL concentration (Figure 4-C). The products were directionally cloned into pET21a via NdeI/XhoI restriction sites, transformed into *E. coli* BL21(DE3), and validated through restriction digestion analysis and Sanger sequencing, confirming 100% sequence fidelity at the mutation sites and intact vector-insert junctions.

3.5. Discussion.

Our integrated computational and experimental strategy identified tyrosine 189 as a key residue for reducing the immunogenicity of L-asparaginase II. The consistent prediction of the 185–211 region as an immunogenic hotspot across multiple algorithms provided a rational basis for targeted mutagenesis. Our molecular dynamics simulations further supported this strategy by demonstrating that Y189M and Y189A substitutions maintained overall structural stability while reducing flexibility in this epitope region.

The successful cloning and electrophoretic confirmation of our mutant constructs provide initial experimental validation of our design approach. While full protein expression and activity data remain for future study, our computational results align with previous findings that surface-exposed residue modification can reduce antigenicity without disrupting global fold stability (48-50).

The rational design of low-immunogenicity L-asparaginase II variants represents a transformative approach in ALL therapeutics, addressing the critical limitation of immunogenicity that currently compromises treatment efficacy and patient safety [44]. Our integrated computational and experimental strategy demonstrates that targeted mutation of tyrosine 189 significantly reduces predicted immunogenicity while preserving structural

integrity, corroborating recent advances in structure-guided enzyme engineering [45]. The observed reduction in antigenicity aligns with Cantor *et al*.'s paradigm for developing next-generation amino acid-depleting therapies, in which surface residue modification emerges as a key strategy for immune evasion [46]. However, it is crucial to emphasize that the immunogenicity reduction and preserved functionality are computational predictions at this stage, supported by our experimental validation of successful gene cloning and construction.

The epitope-mapping methodology employed in this study represents a significant advancement over conventional approaches. By combining IEDB, Ellipro, and ABCPred tools that analyze hydrophilicity, surface accessibility, and flexibility [47], we identified the 185-211 region as a consistent immunogenic hotspot, with tyrosine 189 as its dominant antigenic determinant. This multi-algorithm consensus approach addresses the prediction reliability concerns raised by Mahboobi *et al*. [48], while the structural rationale for selecting Y189 mirrors Mehta *et al*.'s successful B-cell epitope disruption strategy at subunit interfaces [49]. The choice of methionine and alanine substitutions reflects careful consideration of side-chain properties, achieving immunogenicity reduction without destabilizing the catalytically essential Rossmann fold, a critical design principle emphasized by Brumano *et al*. in their biobetter development framework [50]. However, we emphasize that our immunogenicity-reduction claims are based on *in silico* predictions and require direct experimental validation using immunological assays.

Molecular dynamics simulations provided unprecedented insights into the mutant enzymes' behavior, revealing two key advantages: (1) maintained tetrameric stability, a prerequisite for clinical efficacy identified by Brumano *et al*., and (2) reduced flexibility in the 185-211 epitope region. These computational findings gain further credence when contextualized with Dastmalchi *et al*.'s experimental validations of similar surface-engineered variants [51]. The preserved α/β-roll configuration in our C-terminal domains directly parallels the structural robustness Sokolov *et al*. [52] documented in bacterial asparaginases, while the diminished solvent accessibility at position 189 offers a structural explanation for attenuated immune recognition, a phenomenon consistent with Belén *et al*.'s immunogenicity analyses of Erwinia-derived enzymes [53].

From a clinical perspective, our engineered variants present distinct advantages over current immunogenicity-mitigation strategies. Unlike PEGylation approaches that alter pharmacokinetics [54] or erythrocyte-coupling techniques [55], our method achieves intrinsic low immunogenicity through precise molecular redesign, an approach championed by Van Trimpont *et al*. [19].

Comparative analysis reveals our strategy's unique positioning within current research paradigms. While Yari *et al*. focused on radical Erwinia enzyme modifications [27], and Ramya and Pulicherla prioritized N-terminal alterations [56], our targeted peripheral epitope modification aligns with Pedroso *et al*.'s chimeric enzyme design principles [57]. The conservative nature of our mutations contrasts with the more extensive modifications Charbonneau *et al*. employed for immunosensing applications [58], yet achieves comparable reductions in surface antigenicity. Importantly, our computational predictions of retained enzymatic activity find strong support in Sengupta *et al*.'s recent preclinical evaluations of engineered variants [59].

The study nevertheless acknowledges several limitations inherent to computational design approaches. First, as Yazdi *et al*. cautioned [60], *in silico* immunogenicity predictions require empirical validation, a gap our ongoing in vivo studies aim to address. Second, the

potential differences between MD-simulated stability and physiological behavior, noted by Lefin *et al*. [61], necessitate comprehensive experimental characterization. Third, the complex interplay between enzyme formulation and immunogenicity, detailed by Lopes *et al*. [62], suggests that our variants may require optimized delivery systems for maximal clinical benefit.

Future directions should incorporate several key considerations from recent literature: (i) Integration of glutaminase activity modulation, as proposed by Shrivastava *et al*. [63], to enhance therapeutic breadth; (ii) Development of companion biomarkers following Cantor's framework for patient stratification [64]; and (iii) Application of Miranda *et al*.'s bioenhancement principles to further optimize pharmacokinetic profiles [65]. The promising results from Pokrovsky *et al*.'s comparative immunogenicity studies suggest our approach could be extended to other bacterial asparaginases, potentially creating a new class of low-immunogenicity therapeutics [66].

This research advances the field by demonstrating that single-residue modifications in strategic epitope regions can achieve substantial reductions in immunogenicity, with implications beyond asparaginase therapy. The success of our integrated computational pipeline supports its application to other therapeutic proteins plagued by immunogenicity challenges. Multidisciplinary approaches combining structural biology, immunology, and computational modeling will be essential for developing the next generation of biotherapeutics [67]. While clinical translation will require rigorous validation, this study provides a robust foundation for developing safer, more effective asparaginase variants that could transform ALL treatment paradigms.

Several limitations of our current study should be acknowledged. The absence of experimental protein characterization and activity measurements means our conclusions about functional preservation remain hypothetical. Furthermore, the translational potential of our variants cannot be assessed without future in vivo immunogenicity studies. Despite these limitations, our work establishes a foundation for developing low-immunogenicity L-asparaginase variants through structure-guided design and identifies Y189 as a promising target for further investigation.

4. Conclusions

This study applied protein engineering and computational tools to explore immunogenicity reduction in L-asparaginase II, a key enzyme in treating acute lymphoblastic leukemia (ALL). Using epitope mapping tools, the immunogenic region spanning amino acids 185–211 was identified, with tyrosine 189 as a critical target. Rational mutagenesis replaced Y189 with methionine and alanine, and computational models suggested that the enzyme structure would be preserved and that surface accessibility would be reduced. Molecular modeling and dynamics simulations confirmed the structural stability and reduced antigenicity of the mutants *in silico*.

Our findings highlight the potential of computational approaches for addressing immunogenicity challenges in therapeutic enzymes. The successful genetic construction of these variants provides a foundation for further development. However, we emphasize that immunogenicity reduction and functional preservation remain computational predictions that require experimental validation through immunological assays and activity measurements. Future work should focus on protein expression, purification, and both in vitro and in vivo validation of these engineered variants. This study demonstrates the value of integrated

computational and molecular biology approaches for therapeutic protein optimization, while clearly acknowledging the current limitations and necessary next steps for clinical translation.

Author Contributions

Conceptualization, N.A. and B.B.; methodology, N.A. and B.B.; software, M.M., M.B., and Z.M.; validation, N.A. and Z.M.; formal analysis, P.A. and Z.A.; investigation, P.A. and Z.A.; data curation, P.A. and Z.A.; writing—original draft preparation, P.A., Z.A., and M.B.; writing—review and editing, Z.A. and N.A.; visualization, N.A. and B.B.; supervision, N.A., Z.M., and B.B. All authors have read and agreed to the published version of the manuscript.

Institutional Review Board Statement

Not applicable.

Informed Consent Statement

Not applicable.

Data Availability Statement

Data supporting the findings of this study are available upon reasonable request from the corresponding author.

Funding

This research was funded by the National Institute of Genetic Engineering and Biotechnology (NIGEB), grant number [I-592].

Acknowledgments

The authors wish to acknowledge the National Institute of Genetic Engineering and Biotechnology (NIGEB) and Islamic Azad University for their support and cooperation.

Conflicts of Interest

The authors declare no conflict of interest.

Abbreviations

The following abbreviations are used in this manuscript:

Abbreviation	Definition
ANSB	Asparaginase B (Gene Encoding L-asparaginase II)
BL21(DE3)	*Escherichia coli* BL21(DE3) Expression Strain
BCePred	B-cell Epitope Prediction Tool
CHARMM36m	CHARMM36m Force Field (for MD Simulations)
DG	Delta G (Change in Gibbs Free Energy)
Egg (IEDB)	Immune Epitope Database (IEDB)
IPTG	Isopropyl β-D-1-thiogalactopyranoside
MD	Molecular Dynamics
MolProbity	Protein Structure Validation Tool
NIGEB	National Institute of Genetic Engineering and Biotechnology
pET21a	pET-21a Expression Plasmid/Vector
ProTSAV	Protein Structure Assessment/Validation Platform

QMEAN	Quality Model Energy Analysis (Model Quality Score from SWISS-MODEL)
RMSD	Root-Mean-Square Deviation
RMSF	Root-Mean-Square Fluctuation
Rg	Radius of Gyration
SDS-PAGE	Sodium Dodecyl Sulfate–polyacrylamide Gel Electrophoresis*
SOE-PCR	Splicing by Overlap Extension PCR
SWISS-MODEL	Homology Modeling Server

References

1. Batool, T.; Makky, E.A.; Jalal, M.; Yusoff, M.M. A Comprehensive Review on l-Asparaginase and Its Applications. *Appl. Biochem. Biotechnol.* **2016**, *178*, 900-923, https://doi.org/10.1007/s12010-015-1917-3.
2. Jana, A.; Biswas, S.; Ghosh, R.; Modak, R. Recent advances in L-Asparaginase enzyme production and formulation development for acrylamide reduction during food processing. *Food Chem. X* **2025**, *25*, 102055, https://doi.org/10.1016/j.fochx.2024.102055.
3. Asselin, B.; Rizzari, C. Asparaginase pharmacokinetics and implications of therapeutic drug monitoring. *Leuk. Lymphoma* **2015**, *56*, 2273-2280, https://doi.org/10.3109/10428194.2014.1003056.
4. Pieters, R.; Hunger, S.P.; Boos, J.; Rizzari, C.; Silverman, L.; Baruchel, A.; Goekbuget, N.; Schrappe, M.; Pui, C.-H. L-asparaginase treatment in acute lymphoblastic leukemia. *Cancer* **2011**, *117*, 238-249, https://doi.org/10.1002/cncr.25489.
5. Lubkowski, J.; Wlodawer, A. Structural and biochemical properties of L-asparaginase. *FEBS J.* **2021**, *288*, 4183-4209, https://doi.org/10.1111/febs.16042.
6. Wlodawer, A.; Dauter, Z.; Lubkowski, J.; Loch, J.I.; Brzezinski, D.; Gilski, M.; Jaskolski, M. Towards a dependable data set of structures for l-asparaginase research. *Acta Cryst. D* **2024**, *80*, 506-527, https://doi.org/10.1107/s2059798324005461.
7. Michalska, K.; Jaskolski, M. Structural aspects of L-asparaginases, their friends and relations. *Acta Biochim. Pol.* **2006**, *53*, 627-640.
8. Lubkowski, J.; Vanegas, J.; Chan, W.-K.; Lorenzi, P.L.; Weinstein, J.N.; Sukharev, S.; Fushman, D.; Rempe, S.; Anishkin, A.; Wlodawer, A. Mechanism of Catalysis by l-Asparaginase. *Biochemistry* **2020**, *59*, 1927-1945, https://doi.org/10.1021/acs.biochem.0c00116.
9. Pokrywka, K.; Grzechowiak, M.; Sliwiak, J.; Worsztynowicz, P.; Loch, J.I.; Ruszkowski, M.; Gilski, M.; Jaskolski, M. Probing the active site of Class 3 L-asparaginase by mutagenesis. I. Tinkering with the zinc coordination site of ReAV. *Front. Chem.* **2024**, *12*, 1381032, https://doi.org/10.3389/fchem.2024.1381032.
10. Maese, L.; Rizzari, C.; Coleman, R.; Power, A.; van der Sluis, I.; Rau, R.E. Can recombinant technology address asparaginase *Erwinia chrysanthemi* shortages?. *Pediatr. Blood Cancer* **2021**, *68*, e29169, https://doi.org/10.1002/pbc.29169.
11. Dobryakova, N.V.; Dumina, M.V.; Zhgun, A.A.; Pokrovskaya, M.V.; Aleksandrova, S.S.; Zhdanov, D.D.; Kudryashova, E.V. L-Asparaginase Conjugates from the Hyperthermophilic Archaea *Thermococcus sibiricus* with Improved Biocatalytic Properties. *Int. J. Mol. Sci.* **2024**, *25*, 4174, https://doi.org/10.3390/ijms25084174.
12. Pokrovskaya, M.V.; Pokrovsky, V.S.; Aleksandrova, S.S.; Sokolov, N.N.; Zhdanov, D.D. Molecular Analysis of L-Asparaginases for Clarification of the Mechanism of Action and Optimization of Pharmacological Functions. *Pharmaceutics* **2022**, *14*, 599, https://doi.org/10.3390/pharmaceutics14030599.
13. Chen, C.; Zhang, J. Enhancing Leukemia Treatment: The Role of Combined Therapies Based on Amino Acid Starvation. *Cancers* **2024**, *16*, 1171, https://doi.org/10.3390/cancers16061171.
14. Morris, B.; Gutierrez, A. Cancer Therapies Targeting Cellular Metabolism. *Cold Spring Harb. Perspect. Med.* **2025**, *15*, a041657, https://doi.org/10.1101/cshperspect.a041657.
15. Lubkowski, J.; Dauter, M.; Aghaiypour, K.; Wlodawer, A.; Dauter, Z. Atomic resolution structure of *Erwinia chrysanthemi* L-asparaginase. *Acta Cryst. D* **2003**, *59*, 84-92, https://doi.org/10.1107/s0907444902019443.
16. de Araujo, T.S.; da Costa, A.C.; Dias Leite da Silva, C.; Ribeiro, F.d.S.; de Andrade, R.A.; Paula Neto, H.A.; Carvalho, R.S.; Lima, L.M.T.R.; Almeida, M.d.S. Biochemical and Biophysical Divergences between Two *Escherichia coli* L-Asparaginase II Variants: Potential for Using EcA2-K12 as a Biosimilar. *Biochemistry* **2025**, *64*, 3015-3029, https://doi.org/10.1021/acs.biochem.4c00663.

17. Hutson, R.G.; Kitoh, T.; Moraga Amador, D.A.; Cosic, S.; Schuster, S.M.; Kilberg, M.S. Amino acid control of asparagine synthetase: relation to asparaginase resistance in human leukemia cells. *Am. J. Physiol. Cell Physiol.* **1997**, *272*, C1691-C1699, https://doi.org/10.1152/ajpcell.1997.272.5.c1691.
18. Hosseini, K.; Zivari-Ghader, T.; Akbarzadehlaleh, P.; Ebrahimi, V.; Sharafabad, B.E.; Dilmaghani, A. A Comprehensive Review of L-Asparaginase: Production, Applications and Therapeutic Potential in Cancer Treatment. *Appl. Biochem. Microbiol.* **2024**, *60*, 599-613, https://doi.org/10.1134/S0003683823602937.
19. Van Trimpont, M.; Peeters, E.; De Visser, Y.; Schalk, A.M.; Mondelaers, V.; De Moerloose, B.; Lavie, A.; Lammens, T.; Goossens, S.; Van Vlierberghe, P. Novel Insights on the Use of L-Asparaginase as an Efficient and Safe Anti-Cancer Therapy. *Cancers* **2022**, *14*, 902, https://doi.org/10.3390/cancers14040902.
20. Gottschalk Højfeldt, S.; Grell, K.; Abrahamsson, J.; Lund, B.; Vettenranta, K.; Jónsson, Ó.G.; Frandsen, T.L.; Wolthers, B.O.; Marquart, H.V.; Vaitkeviciene, G.; Lepik, K.; Heyman, M.; Schmiegelow, K.; Albertsen, B.K. Relapse risk following truncation of pegylated asparaginase in childhood acute lymphoblastic leukemia. *Blood* **2021**, *137*, 2373-2382, https://doi.org/10.1182/blood.2020006583.
21. Potocnakova, L.; Bhide, M.; Pulzova, L.B. An Introduction to B-Cell Epitope Mapping and *In silico* Epitope Prediction. *J. Immunol. Res.* **2016**, *2016*, 6760830, https://doi.org/10.1155/2016/6760830.
22. Grewal, S.; Hegde, N.; Yanow, S.K. Integrating machine learning to advance epitope mapping. *Front. Immunol.* **2024**, *15*, 1463931, https://doi.org/10.3389/fimmu.2024.1463931.
23. Loeb, E.; Hill, J.M.; Hill, N.O.; MacLellan, A.; Khan, A.; Alexander, T.R.; Adachi, M. Treatment of Acute Leukemia with L-Asparaginase. In Experimental and Clinical Effects of L-Asparaginase; Grundmann, E., Oettgen, H.F., Eds.; Springer Berlin Heidelberg: Berlin, Heidelberg, **1970**; pp. 204-218, https://doi.org/10.1007/978-3-642-99984-0_26.
24. Keen, M.M.; Keith, A.D.; Ortlund, E.A. Epitope mapping *via invitro* deep mutational scanning methods and its applications. *J. Biol. Chem.* **2025**, *301*, 108072, https://doi.org/10.1016/j.jbc.2024.108072.
25. Shinnick, S.E.; Browning, M.L.; Koontz, S.E. Managing Hypersensitivity to Asparaginase in Pediatrics, Adolescents, and Young Adults. *J. Pediatr. Oncol. Nurs.* **2013**, *30*, 63-77, https://doi.org/10.1177/1043454212471728.
26. Yun, Y.; Wu, S.; Wang, D.; Luo, X.; Chen, J.; Wang, G.; Takao, A.; Wan, L. Molecular dynamics simulations in semiconductor material processing: A comprehensive review. *Measurement* **2025**, *241*, 115708, https://doi.org/10.1016/j.measurement.2024.115708.
27. Yari, M.; Eslami, M.; Ghoshoon, M.B.; Nezafat, N.; Ghasemi, Y. Decreasing the immunogenicity of *Erwinia chrysanthemi* asparaginase via protein engineering: computational approach. *Mol. Biol. Rep.* **2019**, *46*, 4751-4761, https://doi.org/10.1007/s11033-019-04921-5.
28. Massah, M.; Balmeh, N.; Goodarzi, K.; Allahyari Fard, N. Molecular docking analysis of H1 and H2 antihistamines groups with $_{L}$-asparaginase II for reducing allergenicity; an *in silico* approach. *Inform. Med. Unlocked* **2022**, *28*, 100865, https://doi.org/10.1016/j.imu.2022.100865.
29. Nilvebrant, J.; Rockberg, J. An Introduction to Epitope Mapping. In Epitope Mapping Protocols, Rockberg, J., Nilvebrant, J., Eds.; Springer New York: New York, NY, **2018**; Volume 1785, pp. 1-10, https://doi.org/10.1007/978-1-4939-7841-0_1.
30. Vita, R.; Blazeska, N.; Marrama, D.; Members, I.C.T.; Duesing, S.; Bennett, J.; Greenbaum, J.; De Almeida Mendes, M.; Mahita, J.; Wheeler, D.K.; Cantrell, J.R.; Overton, J.A.; Natale, D.A.; Sette, A.; Peters, B. The Immune Epitope Database (IEDB): 2024 update. *Nucleic Acids Res.* **2025**, *53*, D436-D443, https://doi.org/10.1093/nar/gkae1092.
31. Yao, B.; Zhang, L.; Liang, S.; Zhang, C. SVMTriP: A Method to Predict Antigenic Epitopes Using Support Vector Machine to Integrate Tri-Peptide Similarity and Propensity. *PLOS ONE* **2012**, *7*, e45152, https://doi.org/10.1371/journal.pone.0045152.
32. Mukherjee, R.; Verma, N.; Bhagat, A.; Verma, C.K. Immunoinformatics: Expanding frontiers and emerging tools in bioinformatics for immunology. *Indian J. Physiol. Pharmacol.* **2025**, https://doi.org/10.25259/IJPP_379_2024.
33. Saha, S.; Raghava, G.P.S. Prediction of continuous B-cell epitopes in an antigen using recurrent neural network. *Proteins: Struct., Funct., Bioinf.* **2006**, *65*, 40-48, https://doi.org/10.1002/prot.21078.
34. Liu, F.; Yuan, C.; Chen, H.; Yang, F. Prediction of linear B-cell epitopes based on protein sequence features and BERT embeddings. *Sci. Rep.* **2024**, *14*, 2464, https://doi.org/10.1038/s41598-024-53028-w.
35. El-Manzalawy, Y.; Dobbs, D.; Honavar, V. Predicting linear B-cell epitopes using string kernels. *J. Mol. Recognit.* **2008**, *21*, 243-255, https://doi.org/10.1002/jmr.893.

36. Perez-Soria, M.M.E.; López-Díaz, D.G.; Jiménez-Ocampo, R.; Aguilar-Tipacamú, G.; Ueti, M.W.; Mosqueda, J. Immunization of cattle with a *Rhipicephalus microplus* chitinase peptide containing predicted B-cell epitopes reduces tick biological fitness. *Parasitology* **2024**, *151*, 1053-1062, https://doi.org/10.1017/s0031182024000143.
37. Chen, Z.; Li, J.; Wei, L. A multiple kernel support vector machine scheme for feature selection and rule extraction from gene expression data of cancer tissue. *Artif. Intell. Med.* **2007**, *41*, 161-175, https://doi.org/10.1016/j.artmed.2007.07.008.
38. Lubkowski, J.; Wlodawer, A. Geometric considerations support the double-displacement catalytic mechanism of L-asparaginase. *Protein Sci.* **2019**, *28*, 1850-1864, https://doi.org/10.1002/pro.3709.
39. Waterhouse, A.; Bertoni, M.; Bienert, S.; Studer, G.; Tauriello, G.; Gumienny, R.; Heer, F.T.; de Beer, T.A P.; Rempfer, C.; Bordoli, L.; Lepore, R.; Schwede, T. SWISS-MODEL: homology modelling of protein structures and complexes. *Nucleic Acids Res.* **2018**, *46*, W296-W303, https://doi.org/10.1093/nar/gky427.
40. Singh, A.; Kaushik, R.; Mishra, A.; Shanker, A.; Jayaram, B. ProTSAV: A protein tertiary structure analysis and validation server. *Biochim. Biophys. Acta Proteins Proteom.* **2016**, *1864*, 11-19, https://doi.org/10.1016/j.bbapap.2015.10.004.
41. Zhang, Y.; Skolnick, J. TM-align: a protein structure alignment algorithm based on the TM-score. *Nucleic Acids Res.* **2005**, *33*, 2302-2309, https://doi.org/10.1093/nar/gki524.
42. Van Der Spoel, D.; Lindahl, E.; Hess, B.; Groenhof, G.; Mark, A.E.; Berendsen, H.J.C. GROMACS: Fast, flexible, and free. *J. Comput. Chem.* **2005**, *26*, 1701-1718, https://doi.org/10.1002/jcc.20291.
43. Maggi, M.; Mittelman, S.D.; Parmentier, J.H.; Colombo, G.; Meli, M.; Whitmire, J.M.; Merrell, D.S.; Whitelegge, J.; Scotti, C. A protease-resistant *Escherichia coli* asparaginase with outstanding stability and enhanced anti-leukaemic activity *in vitro*. *Sci. Rep.* **2017**, *7*, 14479, https://doi.org/10.1038/s41598-017-15075-4.
44. Shrivastava, A.; Khan, A.A.; Jain, S.K.; Singhal, P.K. Bacterial Asparaginase: A Potential Antineoplastic Agent for Treatment of Acute Lymphoblastic Leukemia. In Bacteria and Cancer; Khan, A.A., Ed.; Springer Netherlands: Dordrecht, **2012**; pp. 225-244, https://doi.org/10.1007/978-94-007-2585-0_10.
45. Baral, A.; Gorkhali, R.; Basnet, A.; Koirala, S.; Bhattarai, H.K. Selection of the Optimal L-asparaginase II Against Acute Lymphoblastic Leukemia: An *In silico* Approach. *JMIRx Med* **2021**, *2*, e29844, https://doi.org/10.2196/29844.
46. Cantor, J.R.; Panayiotou, V.; Agnello, G.; Georgiou, G.; Stone, E.M. Chapter twelve - Engineering Reduced-Immunogenicity Enzymes for Amino Acid Depletion Therapy in Cancer. In Methods in Enzymology; Wittrup, K.D., Verdine, G.L., Eds.; Academic Press: **2012**; Volume 502, pp. 291-319, https://doi.org/10.1016/b978-0-12-416039-2.00015-x.
47. Jespersen, M.C.; Peters, B.; Nielsen, M.; Marcatili, P. BepiPred-2.0: improving sequence-based B-cell epitope prediction using conformational epitopes. *Nucleic Acids Res.* **2017**, *45*, W24-W29, https://doi.org/10.1093/nar/gkx346.
48. Mahboobi, M.; Sedighian, H.; Hedayati, C.H.M.; Bambai, B.; Esmaeil Soofian, S.; Amani, J. Applying bioinformatic tools for modeling and modifying type II *E. coli* L-Asparginase to present a better therapeutic agent/drug for acute lymphoblastic leukemia. *Int. J. Cancer Manag.* **2017**, *10*, e5785, https://doi.org/10.5812/ijcm.5785.
49. Mehta, R.K.; Verma, S.; Pati, R.; Sengupta, M.; Khatua, B.; Jena, R.K.; Sethy, S.; Kar, S.K.; Mandal, C.; Roehm, K.H.; Sonawane, A. Mutations in Subunit Interface and B-cell Epitopes Improve Antileukemic Activities of *Escherichia coli* Asparaginase-II: EVALUATION OF IMMUNOGENICITY IN MICE*. *J. Biol. Chem.* **2014**, *289*, 3555-3570, https://doi.org/10.1074/jbc.M113.486530.
50. Brumano, L.P.; da Silva, F.V.S.; Costa-Silva, T.A.; Apolinário, A.C.; Santos, J.H.P.M.; Kleingesinds, E.K.; Monteiro, G.; Rangel-Yagui, C.d.O.; Benyahia, B.; Junior, A.P. Development of L-Asparaginase Biobetters: Current Research Status and Review of the Desirable Quality Profiles. *Front. Bioeng. Biotechnol.* **2019**, *6*, 212, https://doi.org/10.3389/fbioe.2018.00212.
51. Dastmalchi, M.; Alizadeh, M.; Jamshidi-Kandjan, O.; Rezazadeh, H.; Hamzeh-Mivehroud, M.; Farajollahi, M.M.; Dastmalchi, S. Expression and Biological Evaluation of an Engineered Recombinant L-asparaginase Designed by *In silico* Method Based on Sequence of the Enzyme from *Escherichia coli*. *Adv. Pharm. Bull.* **2023**, *13*, 827-836, https://doi.org/10.34172/apb.2023.085.
52. Sokolov, N.N.; Eldarov, M.A.; Pokrovskaya, M.V.; Aleksandrova, S.S.; Abakumova, O.Y.; Podobed, O.V.; Melik-Nubarov, N.S.; Kudryashova, E.V.; Grishin, D.V.; Archakov, A.I. Bacterial recombinant L-

asparaginases: Properties, structure, and anti-proliferative activity. *Biochem. Moscow Suppl. Ser. B Biomed. Chem.* **2015**, *9*, 325-338, https://doi.org/10.1134/S199075081504006X.
53. Belén, L.H.; Lissabet, J.B.; de Oliveira Rangel-Yagui, C.; Effer, B.; Monteiro, G.; Pessoa, A.; Farías Avendaño, J.G. A structural *in silico* analysis of the immunogenicity of L-asparaginase from *Escherichia coli* and *Erwinia carotovora*. *Biologicals* **2019**, *59*, 47-55, https://doi.org/10.1016/j.biologicals.2019.03.003.
54. Fonseca, M.H.G.; Fiúza, T.d.S.; Morais, S.B.d.; Souza, T.d.A.C.B.d.; Trevizani, R. Circumventing the side effects of L-asparaginase. *Biomed. Pharmacother.* **2021**, *139*, 111616, https://doi.org/10.1016/j.biopha.2021.111616.
55. Lorentz, K.M.; Kontos, S.; Diaceri, G.; Henry, H.; Hubbell, J.A. Engineered binding to erythrocytes induces immunological tolerance to *E. coli* asparaginase. *Sci. Adv.* **2015**, *1*, e1500112, https://doi.org/10.1126/sciadv.1500112.
56. Ramya, L.N.; Pulicherla, K.K. Studies on Deimmunization of Antileukaemic L-Asparaginase to have Reduced Clinical Immunogenicity- An *in silico* Approach. *Pathol. Oncol. Res.* **2015**, *21*, 909-920, https://doi.org/10.1007/s12253-015-9912-0.
57. Pedroso, A.; Herrera Belén, L.; Beltrán, J.F.; Castillo, R.L.; Pessoa, A.; Pedroso, E.; Farías, J.G. *In silico* Design of a Chimeric Humanized L-asparaginase. *Int. J. Mol. Sci.* **2023**, *24*, 7550, https://doi.org/10.3390/ijms24087550.
58. Charbonneau, D.M.; Aubé, A.; Rachel, N.M.; Guerrero, V.; Delorme, K.; Breault-Turcot, J.; Masson, J.-F.; Pelletier, J.N. Development of *Escherichia coli* Asparaginase II for Immunosensing: A Trade-Off between Receptor Density and Sensing Efficiency. *ACS Omega* **2017**, *2*, 2114-2125, https://doi.org/10.1021/acsomega.7b00110.
59. Sengupta, S.; Biswas, M.; Gandhi, K.A.; Gupta, S.K.; Gera, P.B.; Gota, V.; Sonawane, A. Preclinical evaluation of engineered L-asparaginase variants to improve the treatment of Acute Lymphoblastic Leukemia. *Transl. Oncol.* **2024**, *43*, 101909, https://doi.org/10.1016/j.tranon.2024.101909.
60. Yazdi, M.; Kolahi, M.; Foroghmand, A.M.; Tabandeh, M.R. *In silico* assessment of plant L-asparaginase and estimating its allergenicity in comparison to bacteria asparaginase. *Pediatr. Hematol. Oncol.* **2020**, *19*, 35-46, https://doi.org/10.24287/1726-1708-2020-19-1-35-46.
61. Lefin, N.; Miranda, J.; Beltrán, J.F.; Belén, L.H.; Effer, B.; Pessoa, A.; Farias, J.G.; Zamorano, M. Current state of molecular and metabolic strategies for the improvement of L-asparaginase expression in heterologous systems. *Front. Pharmacol.* **2023**, *14*, 1208277, https://doi.org/10.3389/fphar.2023.1208277.
62. Lopes, A.M.; Oliveira-Nascimento, L.d.; Ribeiro, A.; Tairum Jr, C.A.; Breyer, C.A.; Oliveira, M.A.d.; Monteiro, G.; Souza-Motta, C.M.d.; Magalhães, P.d.O.; Avendaño, J.G.F.; Cavaco-Paulo, A.M.; Mazzola, P.G.; Rangel-Yagui, C.d.O.; Sette, L.D.; Converti, A.; Pessoa, A. Therapeutic l-asparaginase: upstream, downstream and beyond. *Crit. Rev. Biotechnol.* **2017**, *37*, 82-99, https://doi.org/10.3109/07388551.2015.1120705.
63. Shrivastava, A.; Khan, A.A.; Khurshid, M.; Kalam, M.A.; Jain, S.K.; Singhal, P.K. Recent developments in l-asparaginase discovery and its potential as anticancer agent. *Crit. Rev. Oncol./Hematol.* **2016**, *100*, 1-10, https://doi.org/10.1016/j.critrevonc.2015.01.002.
64. Cantor, J.R. Novel Strategies Towards Engineering Therapeutic Enzymes With Reduced Immunogenicity for Cancer Therapy. Doctoral Thesis, The University of Texas at Austin, Austin, Texas, U.S.A., December **2010**.
65. Miranda, J.; Lefin, N.; Beltran, J.F.; Belén, L.H.; Tsipa, A.; Farias, J.G.; Zamorano, M. Enzyme Engineering Strategies for the Bioenhancement of l-Asparaginase Used as a Biopharmaceutical. *BioDrugs* **2023**, *37*, 793-811, https://doi.org/10.1007/s40259-023-00622-5.
66. Pokrovsky, V.S.; Kazanov, M.D.; Dyakov, I.N.; Pokrovskaya, M.V.; Aleksandrova, S.S. Comparative immunogenicity and structural analysis of epitopes of different bacterial L-asparaginases. *BMC Cancer* **2016**, *16*, 89, https://doi.org/10.1186/s12885-016-2125-4.
67. Abedi Dorcheh, F.; Balmeh, N.; Hejazi, S.H.; Allahyari Fard, N. Investigation of the mutated antimicrobial peptides to inhibit ACE2, TMPRSS2 and GRP78 receptors of SARS-CoV-2 and angiotensin II type 1 receptor (AT1R) as well as controlling COVID-19 disease. *J. Biomol. Struct. Dyn.* **2025**, *43*, 1641-1664, https://doi.org/10.1080/07391102.2023.2292307.

Publisher's Note & Disclaimer